Comprehensive Journal of Science
Volume (10), Issue (37), (NOV. 2025)
SICST2025, www.sicst.ly
ISSN: 3014-6266

مجلة العلوم الشاملة
عدد خاص بالمؤتمر الدولي الثالث للعلوم والتقنية
المجلد (10)، العدد (37)، (نوفمبر2025)
ردمد: 3014-6266

Fabrication and Evaluating Cellulose Acetate Flat-Sheet FO Membranes with Ionic-Liquid ([HBet][Tf_2N]) and Inorganic (NaCl, $MgCl_2$) Draw Solutions

Saber Abdulhamid Alftessi [1*], Mohamed Farag Twibi[1], Husein D. Meshreghi[2], Abdulghani Swesi[1],
Jamal Amar Ashour Eljourni[1]
[1] Chemical technology, Higher Institute of Science and Technology Soqalkhamis Imsehel, Tripoli, Libya
[2] Energy Engineering Department, College of Renewable Energy, Tajoura, Tripoli, Libya
*Corresponding author: ftc9170@gmail.com

تصنيع وتقييم أغشية التناضح الأمامي المسطّحة المصنوعة من أسيتات السليلوز باستخدام محاليل سحب أيونية ([HBet][Tf_2N]) وغير عضوية ($MgCl_2$, NaCl)

صابر عبد الحميد الفطيسي[1*]، محمد فرج الطويبي[1]، حسين الضاوي المشرقي[2]، عبد الغني السويسي[1]، جمال عمار الزايدي[1]
[1] قسم التقنية الكيميائية، المعهد العالي للعلوم والتقنية (سوق الخميس امسيحل) طرابلس /ليبيا
[2] قسم هندسة الطاقة، كلية الطاقات المتجددة تاجوراء/طرابلس/ ليبيا

Received: 30-09-2025; Revised: 10-10-2025; Accepted: 31-10-2025; Published: 25-11-2025

Abstract:

Forward osmosis (FO) has emerged as a highly attractive separation process for water desalination due to its reliance on natural osmotic pressure gradients rather than high external hydraulic pressures. In FO, water molecules spontaneously diffuse from a dilute feed solution toward a concentrated draw solution through a semi-permeable membrane that selectively permits water transport while rejecting solutes. In the present investigation, cellulose acetate (CA) flat-sheet membranes were prepared with two different polymer loadings (20 wt.% and 25 wt.%) in order to assess the relationship between membrane structure and FO performance. Experimental results revealed that lowering the polymer concentration significantly enhanced water flux, albeit at the expense of reduced solute rejection, underscoring the classical permeability–selectivity trade-off. Furthermore, the influence of thermal conditioning through a two-step heat treatment (20 min at 60 °C and 90 °C) was systematically analyzed. The untreated CA membrane achieved the highest water flux of 1.48 $L\cdot m^{-2}\cdot h^{-1}$, in contrast to 1.254 $L\cdot m^{-2}\cdot h^{-1}$ and 1.006 $L\cdot m^{-2}\cdot h^{-1}$ for membranes subjected to 60 °C and 90 °C treatment, respectively, highlighting the flux decline induced by thermal densification of the polymer matrix. Remarkably, the CA-0 membrane exhibited superior water permeation when paired with the UCST ionic liquid ([Hbet][Tf_2N]) as the draw solution. Within 30 seconds, approximately 7.0 g of feed water was transported across the membrane, outperforming conventional inorganic salts such as NaCl (6.33 g) and $MgCl_2$ (4.12 g) under identical operating conditions. These findings confirm that the UCST ionic liquid offers a stronger osmotic driving force, thereby achieving superior flux performance and demonstrating its potential as a next-generation draw agent for FO desalination.

Keywords: Cellulose acetate (CA); Forward osmosis (FO); Ionic liquid ([Hbet][Tf_2N]); Heat treatment.

الملخص:

أصبح التناضح الأمامي (FO) في الآونة الأخيرة أحد أكثر تقنيات الفصل الواعدة في مجال تحلية المياه، وذلك لاعتماده على فروق الضغط الاسموزي الطبيعية بدلًا من الحاجة إلى ضغوط هيدروليكية مرتفعة. يقوم مبدأ العملية على انتقال جزيئات الماء تلقائيًا من محلول مغذٍ منخفض التركيز إلى محلول سحب عالي التركيز عبر غشاء شبه منفذ يسمح بمرور الماء ويمنع مرور الأملاح. في هذه الدراسة، جرى تحضير أغشية مسطحة من أسيتات السليلوز (CA) بتركيزين بوليمريين مختلفين (20% و25% وزناً) بهدف تقييم العلاقة بين البنية الغشائية وأداء FO. أظهرت النتائج أن تقليل تركيز البوليمر يؤدي إلى زيادة ملحوظة في تدفق المياه، ولكن على حساب انخفاض كفاءة رفض الأملاح، مما يعكس المفاضلة التقليدية بين النفاذية والانتقائية. كما تم تحليل تأثير المعالجة الحرارية المزدوجة (20 دقيقة عند 60 °م و90 °م) بصورة منهجية. حقق الغشاء غير المعالج أعلى تدفق مائي بلغ 1.48 لتر·م$^{-2}$·ساعة$^{-1}$، مقارنةً بـ 1.254 لتر·م$^{-2}$·ساعة$^{-1}$ و1.006 لتر·م$^{-2}$·ساعة$^{-1}$ للأغشية المعالجة عند 60 °م و90 °م على التوالي، وهو ما يبرز الانخفاض في التدفق الناتج عن تكثيف مصفوفة البوليمر بفعل الحرارة. ومن الجدير بالذكر أن الغشاء (CA–0) أظهر نفاذية مائية متفوقة عند استخدام السائل الأيوني ([Hbet][Tf_2N]) عند درجة الحرارة الحرجة العليا (UCST) كمحلول سحب. ففي غضون 30 ثانية، تم نقل ما يقارب 7.0 غرام من ماء التغذية عبر الغشاء، متفوقًا على محاليل الأملاح غير العضوية التقليدية مثل NaCl (6.33 غ) و $MgCl_2$(4.12 غ) تحت نفس الظروف التشغيلية. تؤكد هذه النتائج أن السائل الأيوني عند UCST يوفّر قوة اسموزية دافعة أعلى، مما يحقق كفاءة تدفق محسّنة ويبرهن على إمكاناته الكبيرة كعامل سحب من الجيل الجديد في تحلية المياه باستخدامFO.

الكلمات المفتاحية: أسيتات السليلوز (CA) ؛ التناضح الأمامي(FO) ؛ السائل الأيوني([Hbet][Tf_2N]) ؛ المعالجة الحرارية.

1 INTRODUCTION

Water scarcity has become a pressing global issue, as many nations lack sufficient resources to meet the growing demands of urban populations, agricultural activities, and natural ecosystems. With freshwater demand rising at an unprecedented rate, addressing this shortage has been recognized as one of the most critical challenges of the twenty-first century (Ward & Pulido-Velazquez 2008). Rapid population growth, coupled with accelerated industrialization, has intensified concerns regarding the sustainability of water resources worldwide. Ensuring adequate water availability is therefore indispensable for safeguarding public health, supporting economic development, and maintaining social stability (Chekli et al. 2012).

Forward osmosis (FO) has emerged as a promising technology capable of addressing these challenges by providing both renewable energy opportunities and access to clean water. Owing to its environmentally friendly and energy-efficient nature, FO is increasingly regarded as a cost-effective solution in the face of mounting global water shortages (Balyan & Sarkar 2015). The process operates on the principle of osmotic pressure differences, whereby water molecules are transported across a semi-permeable membrane from a low-concentration feed solution to a high-concentration draw solution (Cai et al., 2015). This mass transfer results in the feed solution becoming progressively concentrated, while the draw solution is correspondingly diluted, (Akther et al. 2015; Marth 1998). Due to these characteristics, FO has attracted attention across multiple application areas, including seawater and brackish water desalination, wastewater detoxification, high-purity water production, and even energy generation through pressure-retarded osmosis (Cai, Wang, et al. 2015). Collectively, these applications highlight FO's potential as a sustainable and adaptable technology for tackling one of the greatest resource challenges of our time.

The use of thermolytic draw solutes has demonstrated that forward osmosis (FO) can achieve greater energy efficiency and cost-effectiveness in water desalination compared to conventional reverse osmosis (RO) (Minier et al., 2015). The FO process generally involves two fundamental steps: the dilution of a concentrated draw solution through water permeation, followed by the separation and recovery of clean water from the diluted draw solution. The efficiency of an ideal draw solute is therefore determined by its ability to generate high osmotic pressure, provide elevated water flux, ensure safe environmental compatibility (low toxicity), and enable significant recovery of both water and draw solute (Chung et al. 2012). Unlike RO, which relies on the application of high hydraulic pressure to achieve desalination, FO offers a pressure-free alternative.

Designing and fabricating FO membranes with essential features such as antifouling resistance, low production cost, high water permeability, energy efficiency, and enhanced recovery remain critical objectives for advancing this technology. Identifying suitable draw solutes with optimal efficiency is equally crucial. A variety of solute candidates have been investigated with respect to their osmotic performance, water solubility, and regeneration potential for use in FO desalination and purification (Phuntsho et al. 2012). However, one of the most persistent challenges limiting FO commercialization is the energy-intensive step of recovering clean water from the diluted draw solution. Since profitability and scalability of FO systems largely depend on minimizing the energy required for regeneration, the choice of a draw solute with low recovery energy demand becomes a decisive factor (Thompson & Nicoll 2011).

While RO remains a widely applied desalination method, its reliance on high operating pressures, typically ranging between 60 and 80 bar, makes it costly and often impractical for large-scale or remote applications. In contrast, FO operates based on natural osmotic gradients, allowing water to flow spontaneously across a semi-permeable membrane from a saline feed solution into a more concentrated draw solution, without the need for external pressure. For the FO system to function effectively, the draw solution must possess both high solute concentration to sustain water flux and an ability to be regenerated in an energy-efficient manner. Nevertheless, a key limitation of FO lies in the post-process recovery of both the permeated water and the draw solute. Current approaches often require secondary processes such as nanofiltration or RO, which reduce the overall energy advantage of FO. To overcome this bottleneck, research has recently shifted towards novel thermo-responsive ionic liquids (ILs) as potential draw solutes. These ILs exhibit temperature-dependent solubility: at elevated temperatures they dissolve readily in water, creating strong osmotic pressure, while cooling induces phase separation into distinct IL and water layers. This reversible phase behavior allows straightforward regeneration of both water and draw solute with minimal external energy input, representing a significant advancement toward making FO a commercially viable desalination technology.

2 Experimental

2.1 Materials

All chemicals used in this study were of analytical grade and employed without further purification. Betaine hydrochloride (≥98% purity) and lithium bis(trifluoromethanesulfonyl)imide (LiTFSI, ≥98% purity) were purchased from Acros Organics, while sodium chloride (99.5% purity), magnesium chloride (≥95% purity), formamide, and glycerol were obtained from Fisher Scientific. Cellulose acetate (CA) for membrane fabrication was supplied by Sigma-Aldrich (MO, USA), and acetone was procured from R&M Chemicals. All solutions were prepared with laboratory-grade deionized water.

2.2 Preparation of Cellulose Acetate Flat-Sheet Membranes (CAFSM)

Prior to membrane fabrication, the cellulose acetate (CA) powder was oven-dried at 70 °C overnight to ensure complete removal of residual moisture, thereby improving its solubility and consistency during casting. Two distinct dope solutions were formulated, as summarized in Table 1, to investigate the effect of polymer concentration on membrane properties. For each formulation, a pre-weighed amount of CA powder was dissolved in a binary solvent system consisting of acetone and formamide at ambient temperature. The first dope solution (D/S1) contained 25 wt.% CA, 30 wt.% formamide, and 45 wt.% acetone, whereas the second (D/S2) comprised 20 wt.% CA, 31.66 wt.% formamide, and 48.33 wt.% acetone. The dissolution was performed in a 500 mL blue-cap glass bottle tightly sealed with parafilm to minimize acetone evaporation and maintain a constant solvent ratio.

To achieve a homogenous casting solution, the sealed bottle was mounted on a rotator and mixed overnight using an overhead stirrer motor. This continuous agitation facilitated complete polymer dissolution and uniformity of the dope solution. The prepared solution was then cast uniformly onto a clean glass plate using a 200 µm casting knife, producing a thin film of consistent thickness. The casting process was conducted at a speed of 588.33 s^{-1}, with an evaporation time of approximately 3 seconds before immersion. Immediately after casting, the coated glass plate was transferred to a deionized (DI) water coagulation bath, where phase inversion occurred, leading to polymer precipitation and the formation of a flat-sheet CA membrane. This approach ensured the reproducible fabrication of cellulose acetate flat-sheet membranes with controlled thickness, porosity, and morphology, enabling subsequent evaluation under forward osmosis conditions.

Table1: Casting conditions of CA flat sheet membrane.

CA dope solution (wt%)	**D/S1**	**D/S2**
	CA/acetone/formamide (25:45:30)	**CA/acetone/formamide (20:31.66:48.33)**
speed time (sec^{-1})	588.33 sec^{-1}	588.33 sec^{-1}
Evaporation time (sec)	3	3
Precipitation time (sec)	4	4
Casting knife (µm)	200	200

2.3 Synthesis Of the Ionic Liquid Draw Solution

As shown in Figure 1, an aqueous solution of lithium bis(trifluoromethylsulfonyl)imide (LiTFSI) was prepared by dissolving 1 mol (35 g) of the salt in 500 mL of deionized water, and mixed with 250 mL of an aqueous solution containing 1 mol (19.6 g) of betaine hydrochloride. The combined mixture was stirred continuously at room temperature for 24 h to ensure complete reaction before the aqueous phase was separated from the ionic liquid. The resulting ionic phase was washed five times with small portions of deionized water until no chloride impurities were detected. To reduce residual moisture, the ionic phase was evaporated using a rotary evaporator at 60 °C and subsequently dried in a vacuum oven at 120 °C. The final ionic liquid was cooled to room temperature and stored for further use (adapted from (Zhong et al. 2015).

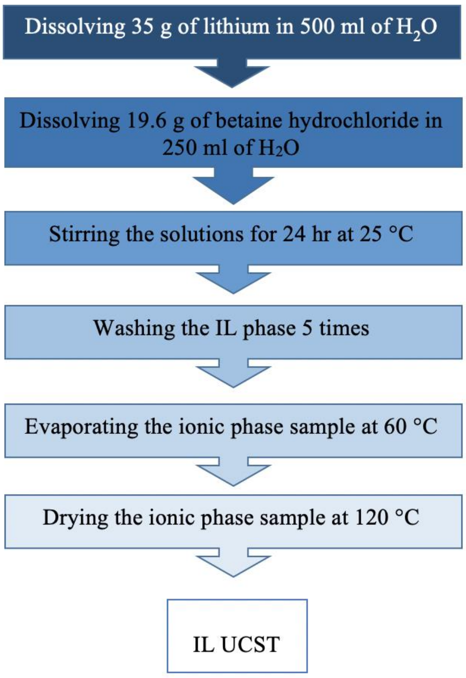

Figure 1: Synthesis of ionic liquid draw solution

2.4 Synthesis of NaCl and $MgCl_2$ Draw Solutions

Magnesium chloride ($MgCl_2$) draw solutions were prepared because of their demonstrated high performance in forward osmosis (FO) treatment processes (Achilli et al. 2010). Precisely 101.65 g, 203.30 g, and 254.12 g of $MgCl_2$ were each dissolved in 500 mL of deionized (DI) water to obtain three concentrations of 1.0 M, 2.0 M, and 2.5 M, respectively. For the sodium chloride (NaCl) draw solution, 58.40 g of NaCl was dissolved in 500 mL of DI water to prepare a 2.0 M solution.

All draw solutions were freshly prepared immediately prior to FO testing to ensure consistency and reproducibility. These different concentrations were selected to systematically evaluate the influence of osmotic pressure on water flux and reverse solute diffusion during FO experiments.

2.5 Heat-Treatment Of The (CA) Flat Sheet Membranes

Following casting, the CA flat sheet membranes were divided into three groups to evaluate the effect of post-casting thermal conditioning. The first membrane sample (CA-0) received no heat treatment and served as the control. The second sample (CA-60) was immersed in a water bath at 60 °C for 20 minutes, after which the bath and membranes were rapidly cooled to room temperature by adding cold water. The third sample (CA-90) underwent a two-step treatment: it was first subjected to the same 60 °C water bath step as CA-60, then transferred to a 90 °C water bath for 20 minutes, followed by rapid cooling to ambient temperature.

All membranes were subsequently soaked in a 50 wt.% aqueous glycerol solution for 48 hours to prevent pore collapse and then air-dried at room temperature prior to module assembly (Su et al., 2010b). This systematic thermal treatment protocol enabled the investigation of heat-induced structural and performance changes in the fabricated CA membranes.

2.6 Permeation Module

A Sterlitech Clear Cast Acrylic forward osmosis (FO) membrane cell module was employed to conduct all FO experiments under controlled laboratory conditions. This module, illustrated in Figure 2, is specifically designed for bench-scale evaluation of flat-sheet membranes. Its transparent acrylic construction allows direct visual observation of the feed and draw solution channels during operation, facilitating the monitoring of flow behavior and potential fouling events.

The detailed specifications of the module—including channel dimensions, flow path configuration, and active membrane area—are summarized in Table 2. This setup ensured consistent hydrodynamic conditions and reproducible measurements of water flux and solute rejection across the cellulose acetate flat-sheet membranes during testing.

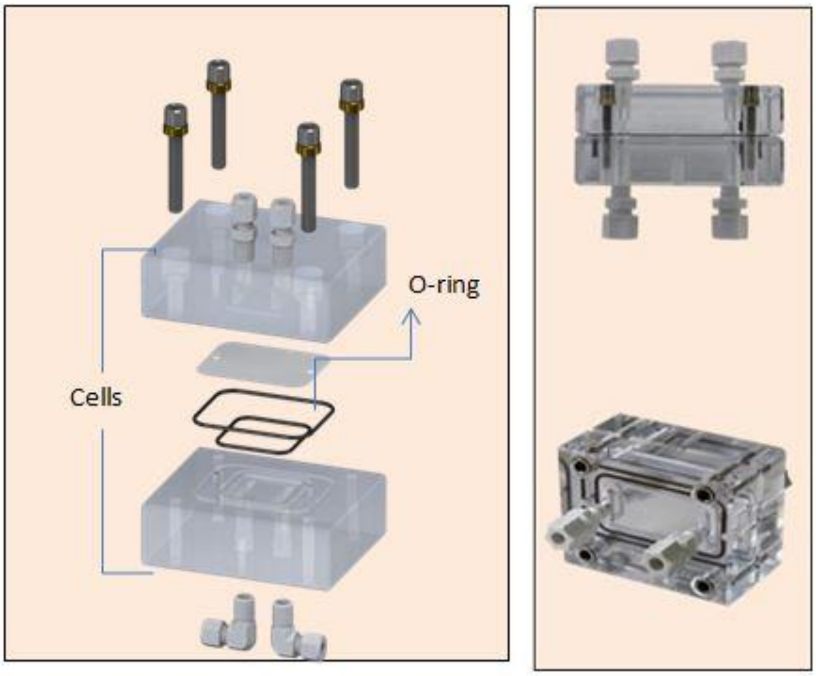

Figure 2: Sterlitech clear cast acrylic FO membrane cells module

Table 2: The general specifications of the clear cast acrylic FO membrane cells

Active Membrane Area	42 cm^2 (6.5 in^2)
Max Temperature	80°C (180°F)
O-Ring	Buna-N
Outer Dimensions	12.7 x 10 x 8.3 cm (5 x 4 x 3.25 in)
Active Area Dimensions	9.207 x 4.572 cm (3.625 x 1.8 in)
Slot Depth	0.23 cm (0.09 in)

2.7 Forward Osmosis Performance Test

Forward osmosis (FO) experiments were conducted at laboratory scale using a Sterlitech Clear Cast Acrylic FO cell module. Prior to assembly, O-rings were carefully installed in the grooves of the cell to ensure a proper seal and prevent leakage during operation. The cellulose acetate (CA) flat-sheet membrane was positioned vertically between the two cells, ensuring it fit precisely over the posts and between the O-rings. The upper cell body was then aligned with the four guideposts and connected to the feed and draw solution vessels, as shown in Figure 3.

During operation, the draw solution flowed through one cell compartment, while the feed solution flowed through the opposite compartment. Water was transported spontaneously through the semi-permeable membrane from the feed solution to the draw solution due to the osmotic pressure difference, resulting in an increase in draw solution volume and a corresponding decrease in feed solution volume (Cai et al. 2015). Consequently, the feed solution became more concentrated while the draw solution became more diluted over time.

The ionic-liquid (IL) draw solution was prepared at 1.0 M, while $MgCl_2$ draw solutions were prepared at 1.0, 2.0, and 2.5 M. The feed solution consisted of 0.6 M NaCl prepared in a 200 mL vessel. To monitor mass changes during the experiment, the feed solution vessel was placed on an electronic balance and weighed continuously. The test was performed for 90 minutes, with mass measurements recorded at 10-minute intervals. Temperature and pressure were maintained at ambient conditions throughout. After completion of each run, the final mass of the feed solution was recorded. The water flux through the membrane was calculated using Equation 1(Mehrparvar et al. 2014):

$$Jw = \frac{\Delta V}{A\,\Delta t} \qquad (1)$$

where ΔV ΔV is the volume of water permeated through the membrane (L), Δt Δt is the time (h), and A A is the effective membrane area (m²).

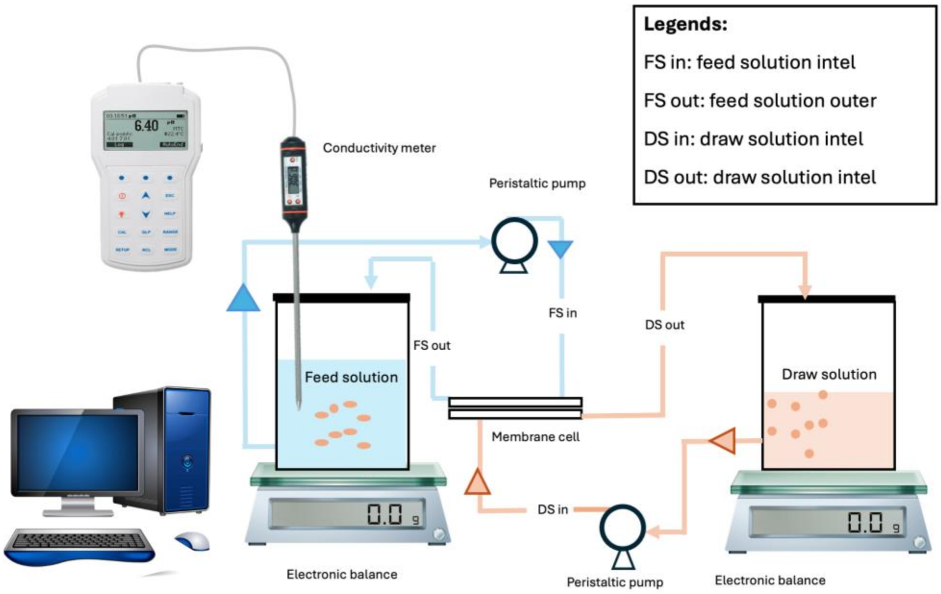

Figure 3 : Setup for FO system

3 Performance tests in FO

3.1 The Effect Of Heat Treatment On Water Flux Of (Nf) Flat Sheet Membrane

Mass transport across the membrane was quantified by measuring the weight change of the feed solution at 10-minute intervals over a 60-minute period, using four types of draw solutions—NaCl (2.0 M), $MgCl_2$ (1.0 M, 2.0 M, 2.5 M), and an ionic liquid (1.0 M)—for the CA-0, CA-60, and CA-90 membranes. As water permeated from the feed solution into the draw solution via osmosis, the weight of the feed solution progressively decreased. Water flux was calculated according to Equation (1). For

NaCl (2.0 M), the highest flux (1.48 L m^{-2} h^{-1}) was recorded for the untreated membrane (CA-0). Flux declined with increasing heat-treatment temperature, decreasing by approximately 0.226 L m^{-2} h^{-1} for the CA-60 membrane treated at 60 °C, while the lowest flux was observed for the CA-90 membrane treated at 90 °C.

This decrease in water flux can be attributed to the higher degree of heat treatment (Idris & Zain 2007). Heat treatment plays a critical role in reducing pore size and densifying the selective layer, which in turn diminishes water permeability. (Idris & Zain 2007), for example, reported that a PES membrane without heat treatment exhibited a pure-water permeation of 14.0 L m^{-2} h^{-1}; when the heat-treatment temperature increased from 50 °C to 150 °C, flux dropped from 12.5 to 4.70 L m^{-2} h^{-1}. The data presented here similarly show that greater heat treatment results in lower flux, consistent with the findings of (Su, Yang, Teo & T. S. Chung 2010). This trend is explained by the fact that the skin layer of the untreated membrane is thinner than that of the heat-treated membranes (Idris & Zain 2007). Thermal annealing has long been recognized as an effective method for modifying the pore structure of polymeric membranes (Kunst & Sourirajan 1970). (Su, Yang, Teo & T. S. Chung 2010) and (Wang et al. 1994) also reported that heat treatment affects not only the surface morphology of CA membranes but also their pore characteristics.

With respect to $MgCl_2$ (1.0 M), the highest water flux reached approximately 1.17 L m^{-2} h^{-1} using the non-thermally treated CA-0 membrane. For the CA-60 membrane heated to 60 °C, the flux decreased to 1.095 L m^{-2} h^{-1}, and it dropped sharply by about 0.137 L m^{-2} h^{-1} for the CA-90 membrane treated at 90 °C, as clearly illustrated in Figure 4.

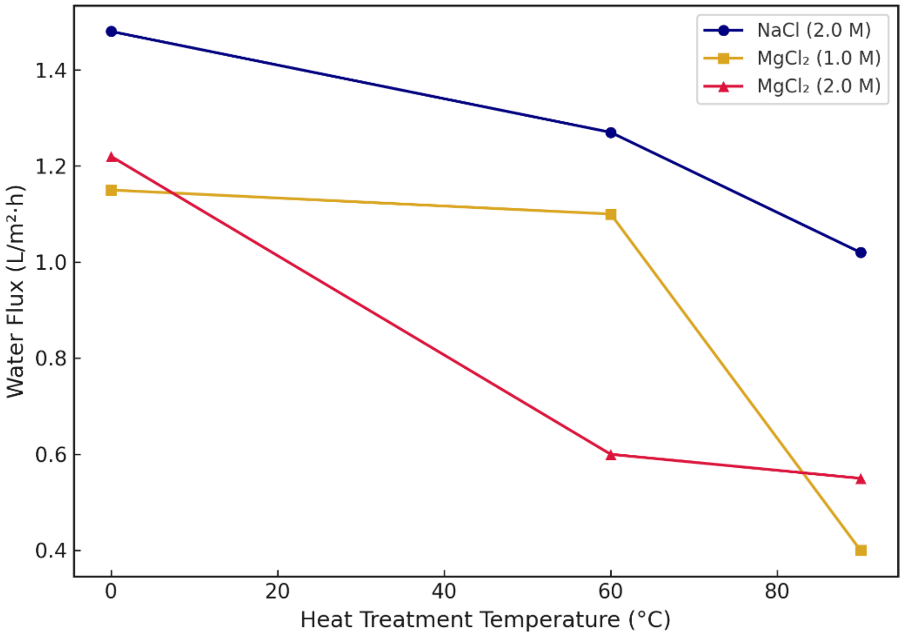

Figure 4: Average of water flux against heat treatment

3.2 Effect of Draw Solution (DS) Concentration on Water Flux

It is well established that increasing the draw solution (DS) concentration enhances water transport across the FO membrane due to a higher osmotic pressure gradient. For example, (Mohd Yusof et al. 2016) reported that water flux increased from 1.3 to 2.3 L m^{-2} h^{-1} when the NaCl DS concentration rose from 0.5 to 2.5 M. A similar trend was observed by (Tang et al. 2010), where water fluxes of 28, 42, and 55 L m^{-2} h^{-1} were achieved at NaCl DS concentrations of 1.0, 2.0, and 3.0 M, respectively.

In the present study, $MgCl_2$ was used as the draw solution at concentrations of 1.0, 2.0, and 2.5 M. As illustrated in Figure 5, the highest water flux of approximately 1.24 L m^{-2} h^{-1} was obtained at 2.5 M, while a flux of 1.22 L m^{-2} h^{-1} was recorded at 2.0 M. The flux continued to decline with decreasing DS concentration. This trend is consistent with previously reported findings, which emphasize that higher DS concentrations produce greater osmotic pressure differences, thereby enhancing water transport through FO membranes.

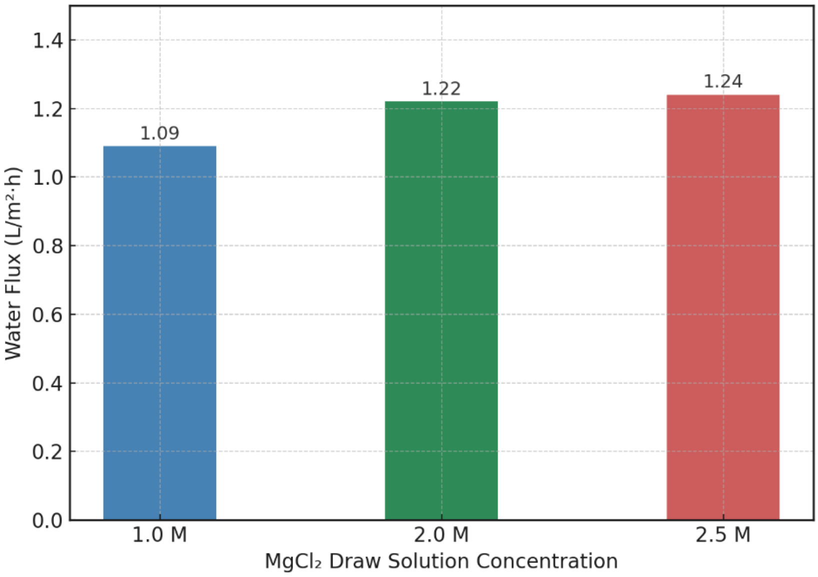

Figure 5*:* The effect of the concentration of DS on water flux

3.3 Performance of the Ionic Liquid (UCST) In Forward Osmosis

As illustrated in Figure 6, the CA-0 membrane exhibited the highest water permeation when the UCST ionic liquid ([Hbet][Tf_2N]) was used as the draw solution. Within 30 seconds, the volume of feed water transported across the membrane reached approximately 7.0 g, compared with 6.33 g for NaCl and 4.12 g for $MgCl_2$ under the same conditions. This clearly indicates that the UCST ionic liquid achieved a superior osmotic driving force, resulting in enhanced flux efficiency relative to the conventional inorganic draw solutions.

This trend of high water flux agrees with the findings of (Zhong et al. 2015), who reported that a 3.2 M solution of protonated betaine bis(trifluoromethylsulfonyl)imide ([Hbet][Tf_2N])—obtained by heating and maintaining the temperature above 56 °C—successfully extracted water from high-salinity solutions up to 3.0 M via FO. The strong osmotic gradient produced by the ionic liquid, combined with its favorable interaction with the membrane, underscores its potential as an advanced draw solution for forward osmosis desalination applications.

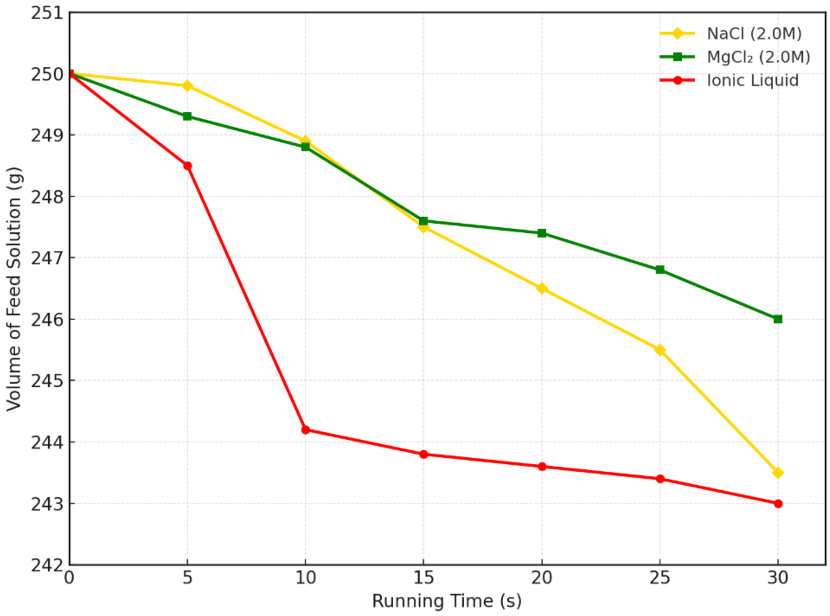

Figure 6: Volume of feed solution against running time using CA-0 membrane

3.4 Effects of Polymer Concentration on Membrane Flux

The concentration of polymer in the casting solution plays a decisive role in determining the structural and transport properties of the resulting membrane. Higher polymer concentrations significantly elevate the viscosity of the dope solution, which slows down the solvent–non-solvent exchange during phase inversion. This slower exchange, coupled with stronger polymer–solvent and polymer–non-solvent interactions, reduces the dissolving power of the solvent and promotes polymer chain entanglement. As a result, denser and less porous membrane structures are formed (Kimmerle & Strathmann 1990).

As illustrated in Figure 7, the membrane cast from 25 wt.% cellulose acetate (CA) using a 2.0 M NaCl draw solution exhibited lower permeability compared to the membrane prepared from 20 wt.% CA. Specifically, the unheated 25 wt.% CA membrane achieved a water flux of 1.48 L m^{-2} h^{-1}, which progressively declined to 1.006 L m^{-2} h^{-1} with heat treatment up to 90 °C. In contrast, the membrane cast from 20 wt.% CA demonstrated a maximum flux of 1.08 L m^{-2} h^{-1}. These findings indicate that higher polymer concentrations result in the formation of thicker and denser skin layers, which increase selectivity but reduce permeability. This trend is consistent with earlier observations reported by (Mustaffar et al. 2004).

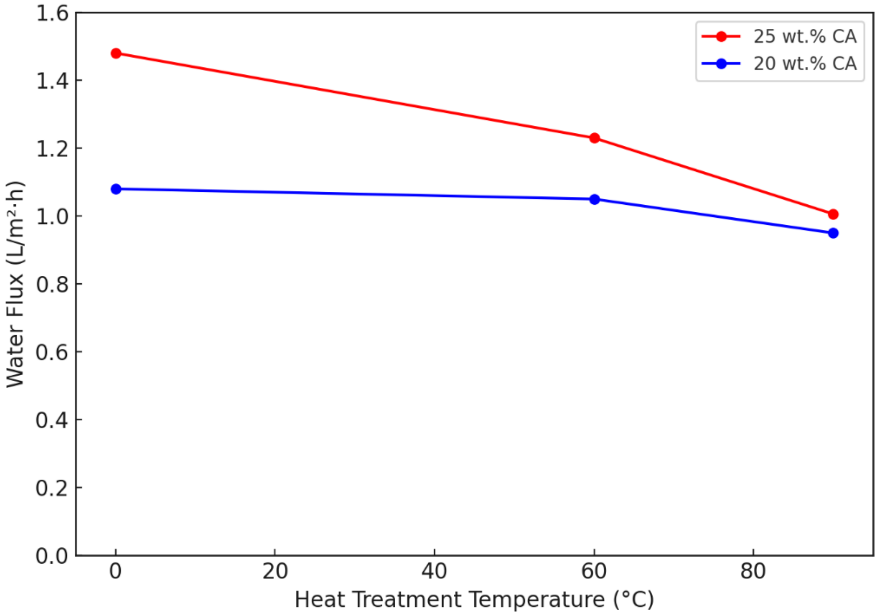

Figure 7: Effects of polymer concentration on membrane flux

3.5 Effects of Heat-Treatment On Salt Flux

Salt flux is defined as the amount of total dissolved solids (TDS) that permeates through a membrane per unit area per unit time. Unlike water flux, salt flux is primarily governed by the concentration gradient across the membrane rather than the applied driving pressure. Table 3 presents the experimental data for water flux and salt flux across the CA-0, CA-60, and CA-90 membranes. The results clearly demonstrate the influence of heat treatment on both water transport and salt leakage.

The untreated membrane (CA-0) exhibited the highest water flux of 1.48 $L/m^2{\cdot}h$. However, this high water transport was accompanied by noticeable salt passage, with a salt flux of 0.479 $g/h{\cdot}m^2$ on the feed side and 0.07 $g/h{\cdot}m^2$ on the draw side. In contrast, the CA-60 membrane, heat-treated at 60 °C, yielded a water flux of 1.254 $L/m^2{\cdot}h$ while significantly reducing salt flux to 0.004 $g/h{\cdot}m^2$. The lowest salt flux was observed in the CA-90 membrane, heat-treated at 90 °C, with a value of only 0.001 $g/h{\cdot}m^2$. These findings indicate that heat treatment reduces both water and salt fluxes, which can be attributed to densification of the selective skin layer and a reduction in effective pore size. This densification improves salt rejection performance, albeit at the expense of water permeability.

Table 3 : Salt and water flux for membranes subjected to different heat-treatment conditions

Membrane	**Feed side**				**Draw side**			
	Concentration M		**Conductivity mS**		**Concentration M**		**Conductivity mS**	
	before	**after**	**before**	**after**	**before**	**after**	**before**	**after**
CA-0	0.6	0.55	60.3	50	2.0	1.945	116.2	140.1
CA-60	0.6	0.6068	60.3	54.013	2.0	1.892	116.2	137.9
CA-90	0.6	0.65	60.3	58.001	2.0	1.8	116.2	133.1

Table 4 : The conductivity and concentration values before and after FO processes

Entry No,	Membrane	Feed side NaCl ($g \cdot L^{-1}$)	Draw side NaCl($g \cdot L^{-1}$)	Water Flux $L/m^2.h$	Salt flux ($g/h.m^2$)	
					Feed side	Draw side
1	CA-0	35.064	116.88	1.48	0.479	0.07
2	CA-60	35.064	116.88	1.254	0.198	0.004
3	CA-90	35.064	116.88	1.006	0.129	0.001

4 CONCLUSION

The performance of cellulose acetate (CA) flat-sheet membranes was systematically investigated for forward osmosis (FO) applications. It was observed that thermal treatment exerts a significant influence on both water flux and salt rejection characteristics of the membranes. Specifically, subjecting the membranes to heat treatment at 90 °C for 20 minutes enhanced NaCl rejection while simultaneously reducing water permeability during FO operations. In contrast, unheated CA nanofiltration (NF) flat-sheet membranes demonstrated high water permeability but exhibited elevated salt flux, indicating a trade-off between selectivity and permeability. Furthermore, an increase in polymer concentration was associated with a decline in the overall performance ratio of the membranes, suggesting a densification effect on the selective layer. The flux ratio was found to rise with higher draw solution concentrations, highlighting the critical role of osmotic driving force in FO performance. Among the draw solutions tested, the UCST ionic liquid (IL) produced the highest water flux when applied to unheated CA flat-sheet membranes, outperforming conventional NaCl and $MgCl_2$ solutions, thereby demonstrating the potential of ILs as effective draw agents for enhancing FO efficiency.

References

Achilli, A., Cath, T. Y., & Childress, A. E. (2010). Selection of inorganic-based draw solutions for forward osmosis applications. *Journal of Membrane Science*, *364*(1–2), 233–241. https://doi.org/10.1016/j.memsci.2010.08.010

Akther, N., Sodiq, A., Giwa, A., Daer, S., Arafat, H. A., & Hasan, S. W. (2015). Recent advancements in forward osmosis desalination : A review. *CHEMICAL ENGINEERING JOURNAL*, *281*, 502–522. https://doi.org/10.1016/j.cej.2015.05.080

Balyan, U., & Sarkar, B. (2015). Enhanced Separation of Polyethylene Glycol from Bovine Serum Albumin Using Electro-Ultrafiltration. *Separation Science and Technology*, *50*(12), 1846–1859. https://doi.org/10.1080/01496395.2015.1014493

Cai, Y., Shen, W., Wei, J., Chong, H., Wang, R., Krantz, W. B., Fane, G., & Hu, X. (2015a). Environmental Science using responsive ionic liquid draw solutes †. *Environmental Science: Water Research & Technology*, *1*, 341–347. https://doi.org/10.1039/C4EW00073K

Cai, Y., Shen, W., Wei, J., Chong, T. H., Wang, R., Krantz, W. B., Fane, A. G., & Hu, X. (2015b). Energy-efficient desalination by forward osmosis using responsive ionic liquid draw solutes. *Environ. Sci.: Water Res. Technol.*, *1*(3), 341–347. https://doi.org/10.1039/C4EW00073K

Cai, Y., Wang, R., Krantz, W. B., Fane, G., & Matthew, X. (2015). RSC Advances Exploration of using thermally responsive polyionic liquid hydrogels as draw agents in forward osmosis †. *RSC Advances*, *5*, 97143–97150. https://doi.org/10.1039/C5RA19018E

Chekli, L., Phuntsho, S., Shon, H. K., Vigneswaran, S., Kandasamy, J., & Chanan, A. (2012). A review of draw solutes in forward osmosis process and their use in modern applications. *Desalination and Water Treatment*, *43*(August 2015), 167–184. https://doi.org/10.1080/19443994.2012.672168

Chung, T.-S., Zhang, S., Wang, K. Y., Su, J., & Ling, M. M. (2012). Forward osmosis processes: Yesterday, today and tomorrow. *Desalination*, *287*(C), 78–81. https://doi.org/10.1016/j.desal.2010.12.019

Idris, A. N. I., & Zain, N. M. A. T. (2007). EFFECT OF HEAT TREATMENT ON THE PERFORMANCE AND STRUCTURAL DETAILS OF POLYETHERSULFONE ULTRAFILTRATION MEMBRANES Membranes with good resistant and selectivity are necessary where efficient separation process is very important for the industrial sector to. *Jurnal Teknologi, 44*, 27–40.

Kimmerle, K., & Strathmann, H. (1990). Analysis of the structure-determining process of phase inversion membranes. *Desalination*, *79*(2–3), 283–302. https://doi.org/10.1016/0011-9164(90)85012-Y

Kunst, B., & Sourirajan, S. (1970). Development and performance of some porous cellulose acetate membranes for reverse osmosis desalination. *Journal of Applied Polymer Science*, *14*(10), 2559–2568. https://doi.org/10.1002/app.1970.070141011

Marth, E. H. (1998). Extended shelf life refrigerated foods: Microbiological quality and safety. *Food Technology*, *52*(2), 57–62. https://doi.org/10.1081/E-EAFE2-120045616

Mehrparvar, A., Rahimpour, A., & Jahanshahi, M. (2014). Modified ultrafiltration membranes for humic acid removal. *Journal of the Taiwan Institute of Chemical Engineers*, *45*(1), 275–282. https://doi.org/10.1016/j.jtice.2013.06.003

Minier-Matar, J., Hussain, A., Santos, A., Janson, A., Wang, R., Fane, A. G., & Adham, S. (2015). Advances in Application of Forward Osmosis Technology for Volume Reduction of Produced/Process Water from Gas-Field Operations. *International Petroleum Technology Conference*. https://doi.org/doi:10.2523/IPTC-18380-MS

Mohd Yusof, M. A., Abu Seman, M. N., & Hilal, N. (2016). Development of polyamide forward osmosis membrane for humic acid removal. *Desalination and Water Treatment*, *3994*(February), 1–5. https://doi.org/10.1080/19443994.2016.1140283

Mustaffar, M. I., Ismail, a. F., & Illias, R. M. (2004). Study on the effect of polymer concentration on hollow fiber ultrafiltration membrane performance and morphology. *Regional Conference on Engineering Education RCEE 2005*, 1–12.

Phuntsho, S., Vigneswaran, S., Kandasamy, J., Hong, S., Lee, S., & Shon, H. K. (2012). Influence of temperature and temperature difference in the performance of forward osmosis desalination process. *Journal of Membrane Science*, *415–416*, 734–744. https://doi.org/10.1016/j.memsci.2012.05.065

Su, J., Yang, Q., Teo, J. F., & Chung, T. S. (2010a). Cellulose acetate nanofiltration hollow fiber membranes for forward osmosis processes. *Journal of Membrane Science*, *355*(1–2), 36–44. https://doi.org/10.1016/j.memsci.2010.03.003

Su, J., Yang, Q., Teo, J. F., & Chung, T.-S. (2010b). Cellulose acetate nanofiltration hollow fiber membranes for forward osmosis processes. *Journal of Membrane Science*, *355*(1), 36–44. https://doi.org/10.1016/j.memsci.2010.03.003

Tang, C. Y., She, Q., Lay, W. C. L., Wang, R., & Fane, A. G. (2010). Coupled effects of internal concentration polarization and fouling on flux behavior of forward osmosis membranes during humic acid filtration. *Journal of Membrane Science*, *354*(1), 123–133. https://doi.org/10.1016/j.memsci.2010.02.059

Thompson, N. A., & Nicoll, P. G. (2011). Forward osmosis desalination: a commercial reality. *IDA World Congress - Perth Convention and Exhibition Centre (PCEC), Perth, Western Australia.*, 16.

Wang, Y., Lau, W. W. Y., & Sourirajan, S. (1994). Effects of pretreatments on morphology and performance of cellulose acetate (formamide type) membranes. *Desalination*, *95*(2), 155–169. https://doi.org/10.1016/0011-9164(94)00011-5

Ward, F. a, & Pulido-Velazquez, M. (2008). Water conservation in irrigation can increase water use. *Proceedings of the National Academy of Sciences of the United States of America*, *105*(47), 18215–18220. https://doi.org/10.1073/pnas.0805554105

Zhong, Y., Feng, X., Chen, W., Wang, X., Huang, K.-W., Gnanou, Y., & Lai, Z. (2015). Using UCST Ionic Liquid as a Draw Solute in Forward Osmosis to Treat High-Salinity Water. *Environmental Science & Technology*, acs.est.5b03747. https://doi.org/10.1021/acs.est.5b03747